Use of computational fluid dynamics in domestic oven design

Mark Fahey#, Sarah J Wakes* and Christopher T Shaw†

*Kahu Technologies, Mosgiel, New Zealand, mark.fahey@kahutech.com
 *Department of Design Studies, University of Otago, PO Box 56, Dunedin, New Zealand, sarah.wakes@design.otago.ac.nz
 †Topajka Shaw Consulting Ltd, 10 Kiwi Burn Place, RD 1 Te Anau, New Zealand, chris.shaw@ihug.co.nz

ABSTRACT

There is an increasing demand, both from customers and regulatory sources, for safer and more energy efficient products. Manufacturers are having to look to their design and development processes to service these demands. Traditional approaches have been to use prototype testing and only delve more deeply into specific aspects of the performance when issues arise. In this work the complex flow within the cooling circuit of the door of a pyrolytic oven is studied. A combination of Computational Fluid Dynamics (CFD) and experimental techniques is used. It will be shown that CFD can help with the achievement of an optimal solution, with the understanding of the flow behaviour and that there is a synergy between the numerical and experimental techniques. Using only one of these techniques would limit the understanding of the flow behaviour and could lead to a less than optimal solution to the design problem. This work aims to explore this particular complex industrial fluid flow situation to:

- · understand the flow around the oven door's cooling circuit
- demonstrate the synergy of CFD and experimental work within development of a complex product
- · explore the role of CFD within the product development process.

Keywords: Computational Fluid Dynamics; Product development; Oven; Experimental methods

1. INTRODUCTION

Increasingly Computational Fluid Dynamics (CFD) is being used within industry to understand and aid the better design of products. There is still a tendency to use CFD to work out why the design did or did not work rather than where in the design space the design will or will not work. This work came out of a larger project based at appliance manufacturer Fisher & Paykel Appliances Ltd in New Zealand. The approach taken was to focus on one complex product in order to explore the fluid and thermal behaviour using CFD. The Titan oven, developed for the US market and being the first oven designed at Fisher & Paykel with a pyrolytic self-cleaning cycle, was chosen to be that focus. It was important with this design that it out-performed competitors products whilst still complying with safety standards, in

particular for the temperature of the oven door during the self-cleaning cycle. The design of the oven had been developed using iterative physical prototypes that allowed a number of design issues to be resolved. It was still felt that the flow around the cooling circuit was illunderstood and an understanding of the flow would be required in order to achieve an optimal solution for future oven designs.

Recent statutory requirements [1] have required manufacturers to display information on the energy usage and efficiency of their product. This has become a point of comparison between competing products and has made manufacturers more aware of how their products function and for ovens, led to a deeper understanding of the thermodynamic behaviour. Compliance with safety regulations is also an important factor in product design and development.

The Titan oven, is a large capacity built-in oven, that has to comply with UL Standards as it is geared to the US market. When this work started the development was well established and therefore there was little chance for the work to assist in the design. What could be done was validate the assumptions made by the development team and point to how CFD could be better utilised for future oven design. The Titan oven was an interesting case for study as it had a pyrolytic self-cleaning cycle where the cavity temperature rises to 500°C for up to 2.5 hours. As the oven has a glass door there has to be a strict safety requirement that the door temperature is no greater than 50°C during this cycle [2, 3].

This work therefore aims to explore this particular complex industrial fluid flow situation to:

- understand the flow around the oven door's cooling circuit
- demonstrate the synergy of CFD and experimental work within the development of a complex product
- explore the role of CFD within the product development process.

2. BACKGROUND

2.1. OVEN DESIGN

There are only a few academic papers concerned with the application of CFD to oven design, in part probably due to commercial sensitivity. CFD has been used in the past to calculate the isothermal, three-dimensional airflow in an industrial, forced convection oven. Although not a domestic food oven, there are still similarities between this and the current work. Verboven et al. modelled the oven cavity, bounded by the inner walls and the door inner surface, [4]. The internal convection fan and heating coils are not modelled explicitly because of their geometric complexity, and neither are the wheeled racks fixed to the sidewalls nor the eight shelves. The fan and heating coils are instead modelled mathematically as a distributed body force and distributed resistance respectively. Turbulence in the flow domain is modelled using the RNG version of the k- ε model with wall functions at the no-slip walls. The model is solved to steady state using a commercial finite volume code on three successively finer grids. The results are validated with experimental hot-wire velocity measurements in the x, y and z directions taken on vertical and horizontal cross-sections of an existing oven, and the maximum velocity is found to be under 6m/s.

A second publication by Verboven et al. [5] considers the same oven, but includes the energy equation in the formulation, leading to predictions of temperatures and heat transfer throughout the cavity. A transient simulation is performed by calculating appropriate heat sources and boundary conditions with a lump model prior to the CFD analysis. The lump model consisted of the different components; air, boundaries, heating coil, door, environment, food and the racks. Given the mass and specific heat capacity of each component and a known heat input to the coils, the temperature of each component was

found by solving a finite element model for the radiation and convection heat transfer between each of the components. Interestingly conduction between the components was not considered and the door was treated as invisible to infrared radiation [6], however good agreement was still found between the lump model and experimental measurements. The time-dependent temperatures of the components and the heat input of the coil became the boundary conditions for the CFD model. The temperatures were assumed uniform over the walls and the value calculated for the food items were specified at the centre. The CFD model simulated the fan-forced airflow and predicted the air temperature distribution and the non-uniform heat transfer rates over the food outer surfaces. Density effects are accounted for through a weakly compressible formulation. Overall the model produced good qualitative insight into the heat distribution during the warm up period. Inaccuracies were attributed to radiation not being included in the CFD model, deficiencies in the turbulence model and wall function, and limitations in grid refinement. Other papers, [7-11], used lump models and empirical models for determining heat loss characteristics and oven performance.

2.2. TURBULENCE MODELLING

Despite its many shortcomings, the RANS approach is commonly used in commercial CFD codes for industrial simulations [12]. It has been validated over a wide range of problems and its deficiencies are well known. The RANS approach is considered as the most practical turbulence handling technique for industrial computational fluid dynamics problems with the computational resources available at the present day [13]. Two-equation eddy viscosity turbulence models have served as the foundation for turbulence research for many years and are used in this work. They offer a good compromise between accuracy and computational effort [12]. Despite the great variety of turbulence modelling options available, the k- ϵ model is unarguably the most widely used and validated two-equation model employed for turbulent fluid dynamics to date [14, 15]. For industrial flows, such as the flow in an oven, the distribution of k and ϵ is seldom known a priori and is often approximated from formulae connecting inlet velocity and a length scale to turbulence production. The extensive use of the k- ϵ model has highlighted both its capabilities and its shortcomings [14]. Its popularity not withstanding, some known limitations of the k- ϵ model include [16]:

- The turbulent kinetic energy is over-predicted in regions of flow impingement and reattachment, leading to poor prediction of the development of flow around leading edges and bluff bodies.
- 2. Regions of re-circulation in a swirling flow are under-estimated.
- 3. Highly swirling flows are generally poorly predicted due to the complex strain fields.
- Mixing is poorly predicted in flows with strong buoyancy effects or high streamline curvature.
- 5. Flow separation from surfaces under the action of adverse pressure gradients is poorly predicted. The real flow is likely to be much closer to separation (or more separated) than the calculations suggest.
- 6. Flow recovery following re-attachment is poorly predicted.
- 7. The spreading rates of wakes and round jets are predicted incorrectly.
- 8. Turbulence driven secondary flows in straight ducts of non-circular cross section are not predicted at all. Linear eddy viscosity models cannot capture this feature.
- 9. Laminar and transitional regions of flow cannot be modelled with the standard k- ε model. This is an active area of research in turbulence modelling.
- 10. Turbulent flows in near-wall regions are not predicted well without special treatment [15].

An alternative two-equation eddy viscosity turbulence model is the k- ω model. In this model the choice for the second variable is the frequency of the vorticity fluctuations, ω . Even though the wall boundary conditions for the k- ω model are more difficult to formulate than for the k- ε , the k- ω model does not require the complex non-linear damping functions for near-wall treatment [12]. It performs well close to walls in boundary layer flows, particularly under strong adverse pressure gradients [17]. However it is very sensitive to the free stream value of ω and unless great care is taken in setting this value, spurious results are obtained in both boundary layer flows and free shear flows [16].

A possible solution to the sensitivity of the k- ω model in the free stream is to use the k- ω model equations in the body of the flow blended into the k- ε turbulence model in the nearwall region. This model is known as the Baseline (BSL) $k-\omega$ model [12] and was developed by Menter [18]. It has been shown to eliminate the free stream sensitivity problem without sacrificing the k- ω 's near-wall performance [16]. The BSL model combines the advantages of the k- ω and the k- ε model, but still fails to properly predict the onset and amount of flow separation from smooth surfaces [12]. The reasons for the deficiency are given in detail by Menter [18], however in summary it stems from the non-equilibrium boundary layer typically found close to separation, causing an imbalance between the turbulence production and dissipation rates, and over-predicting the eddy-viscosity, μ_T . The proper transport behaviour can be obtained by formulating a limiter into the equation for eddy viscosity and accounting for the transportation of shear stress, as is done by the $k-\omega$ based Shear Stress Turbulence (SST) model from Menter [19, 20]. The SST model gives accurate predictions of the onset and the amount of flow separation under adverse pressure gradients. From experience with the SST turbulence model, Menter and Kuntz [21] claim that the capability of the model with respect to the prediction of the onset of separation is within the accuracy of the available experimental data, and that no systematic deviation between the simulations and the data is observed. However there are other effects, which pose additional challenges to the turbulence model, such as the behaviour of the flow downstream of the separation line, including the flow recovery after re-attachment, the proper simulation of vortex flows and questions related to laminar-turbulent transition [21]. The SST model has limited success in these situations.

3. METHODOLOGY

3.1. TITAN OVEN DESIGN

It is important to understand the complexities of the Titan oven's cooling circuit and oven cavity. A design decision was made early in the Titan development to draw the cooling air over the top of the cavity, down the back and out from underneath the cavity as shown in figure 1.

This direction was contrary to existing products but was to prevent hot air being blown into the user's face when the oven is wall mounted. This works against the direction of natural convection in the passage behind the cavity. The cooling airflow through the door enters at the bottom of the door and exits through a vent at the top of the door combining with the main cooling flow around the cavity. The cooling circuit outlet vent is in very close proximity to the inlet vent at the bottom of the door. This raised questions for the engineering team:

- how much of the hot exhaust flow from the oven cooling circuit is recirculating through the door?
- is the flow through the door impeded by low pressure at the bottom of the door created by the Venturi effect from the fast moving exhaust flow?

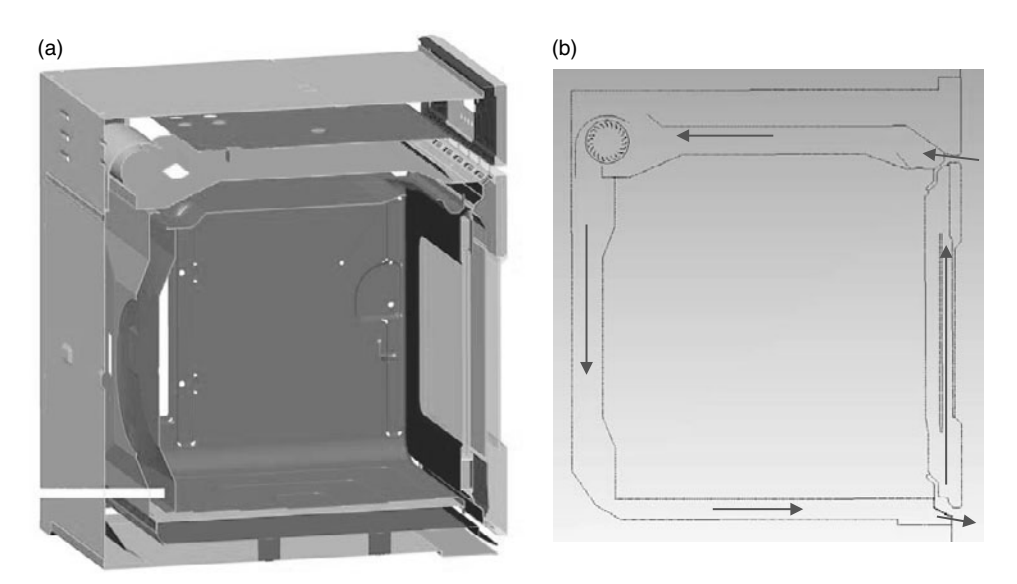


Figure 1 Titan oven. (a) Cross-section. (b) Cooling air path.

Both issues are clearly relevant to the thermal performance of the oven door and highlight the complexity of the issues that arise during development work of this nature. The design was refined by prototype testing until a satisfactory solution was found. Usually during oven development thermal design is not explicitly conducted by numerical or analytical means. The geometric design usually takes precedence over an optimal thermal design provided that the thermal design meets the required performance. Without CFD it was difficult to gain deep understanding of the physical behaviour of the flow in this region.

The five sides of the oven cavity were covered with the maximum thickness of insulation possible. The door on the sixth side provided a more challenging situation. The door was 50mm thick and its design was based on previous experience with other oven doors and by prototype testing. The final design consisted of four panes of glass inside a metal structure. The inner two glass panes next to the cavity had a heat reflective coating to reduce radiation losses and formed a closed cavity with a 4mm thick air gap. The design allowed air to flow through the door between the other panes, thereby reducing the door's external surface temperature. The airflow through the door is in part by natural convection but also by the oven's cooling circuit. The cooling circuit was necessary to carry away excess heat and prevent critical areas such as the door and the electronics from over heating.

A study was undertaken post-launch to study, using CFD, measurement and visualisation techniques, the airflow around the Titan oven cooling circuit and through the oven door. Air is drawn by a tangential fan through an inlet vent between the top of the door and the control panel as shown in figure 2. This airflow combines with air passing through the door and is ducted around the outside of the oven cavity before exhausting from the outlet vent below the door. Immediately adjacent to the outlet vent is an opening at the bottom of the door, figure 3, through which cooling air enters the door.

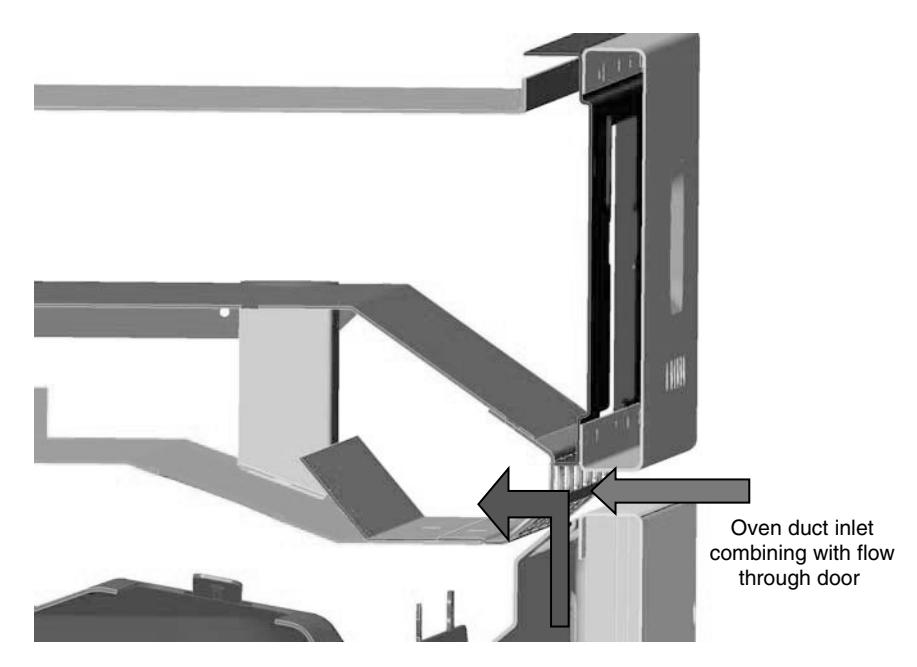


Figure 2 Internal view of inlet at top of oven door.

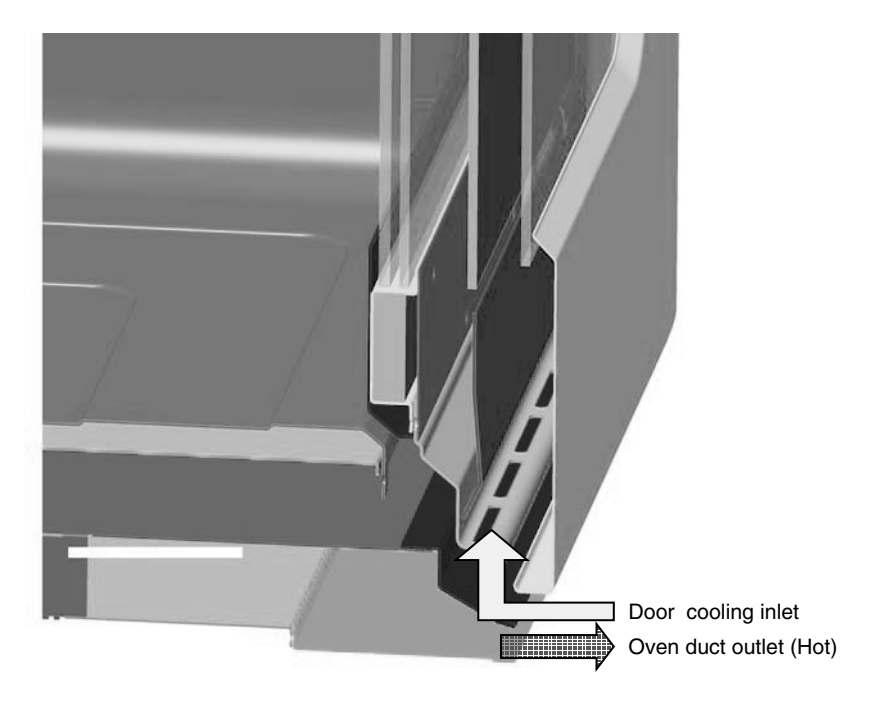


Figure 3 Internal view of bottom of titan oven door.

3.2. FLOW VISUALISATION

Flow visualisation was undertaken to examine the behaviour of the flow at the inlet to the cooling circuit above the door and at the cooling circuit outlet at the bottom of the door. A digital video camera was used to capture the flow, which was seeded with either a fine powder or a water-based oil vapour. A 15mW, 532nm (green) Diode Pumped Solid State (DPSS) laser was used, along with a line-generating lens that changed the beam into a fan-shaped sheet of light, 1mm thick and with a fan angle of 30°. The effectiveness of the flow visualisation technique used here was mixed. It was particularly effective for low-speed, low Reynolds number flows (for example naturally convecting flows), where the concentrations of smoke remained visible for useful periods of time. Many results in these cases were particularly spectacular. In high speed or particularly turbulent flows, such as a fan outlet flow, the smoke became diffused and far larger volumes of smoke were required.

3.3. EXPERIMENTAL MEASUREMENTS

The important parameters were considered to be the temperature around the cooling circuit and the velocities, especially at the inlet and outlet of the cooling circuit. Discrete points were measured in what were considered to be strategic locations.

3.3.1. Temperature

Experiments [22] showed that the standard practice at Fisher & Paykel of attaching thermocouples with aluminium tape was acceptable; however the tape was known to delaminate after lengths of time at moderate temperatures, and quite quickly at elevated temperatures. It was decided therefore to fix the thermocouple to the surface with a small patch of aluminium tape. Under the tape, the thermocouple bead is coated in conductive paste to ensure good thermal contact with the surface being measured. The thermocouple and aluminium patch is then secured with high temperature glue. Within the cavity the thermocouples were fitted by drilling a small hole at the attachment point and clamping the thermocouples under the head of a self-tapping screw. The temperatures were monitored at 59 locations throughout the Titan oven during a pyrolytic self-cleaning cycle.

3.3.2. Velocities

Flow velocities are measured in three regions using hot-wire anemometry. The first set of measurements is taken inside the oven cooling circuit behind the inlet grill. The second set was made at five locations across the width of the outlet vent while the third set was taken from the jet issuing from the cooling circuit outlet vent. The hot-wire measurements were made in ambient air with the oven unheated. The oven was set to tech-mode, which allows individual functions to be controlled, and in this case only the cooling fan was activated. It was necessary to make the hot-wire measurements in ambient air because there were no facilities to calibrate the hot-wire probe in a non-isothermal airflow. Previous work done at Fisher & Paykel indicated that there is very little difference between the flow rates of heated and non-heated air passing around the cooling circuit. Figure 4 shows the locations of the hot-wire measurement points at the inlet with figure 5 showing those at the outlet. The third set of measurement points is shown in figure 6.

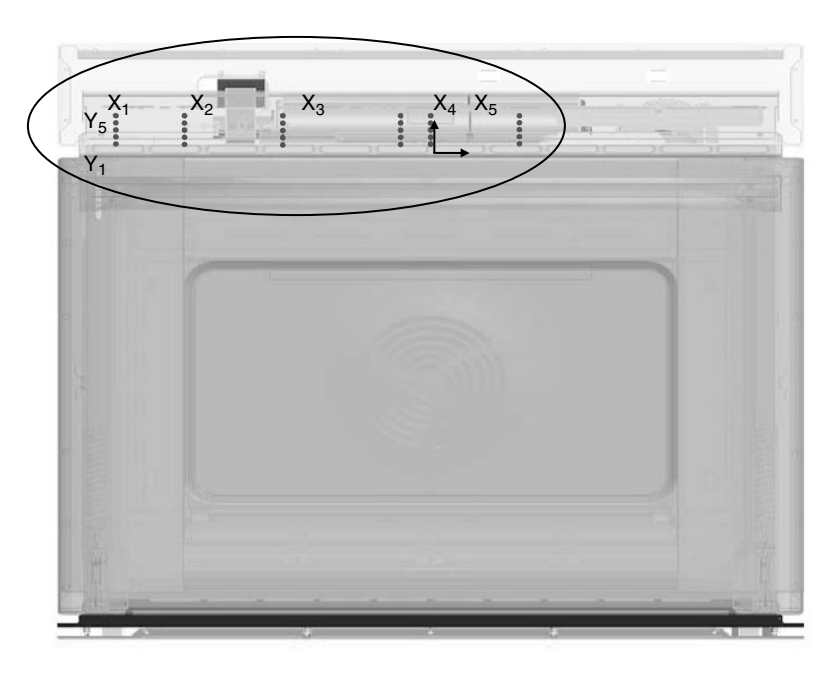


Figure 4 Location of hot-wire measurements at inlet.

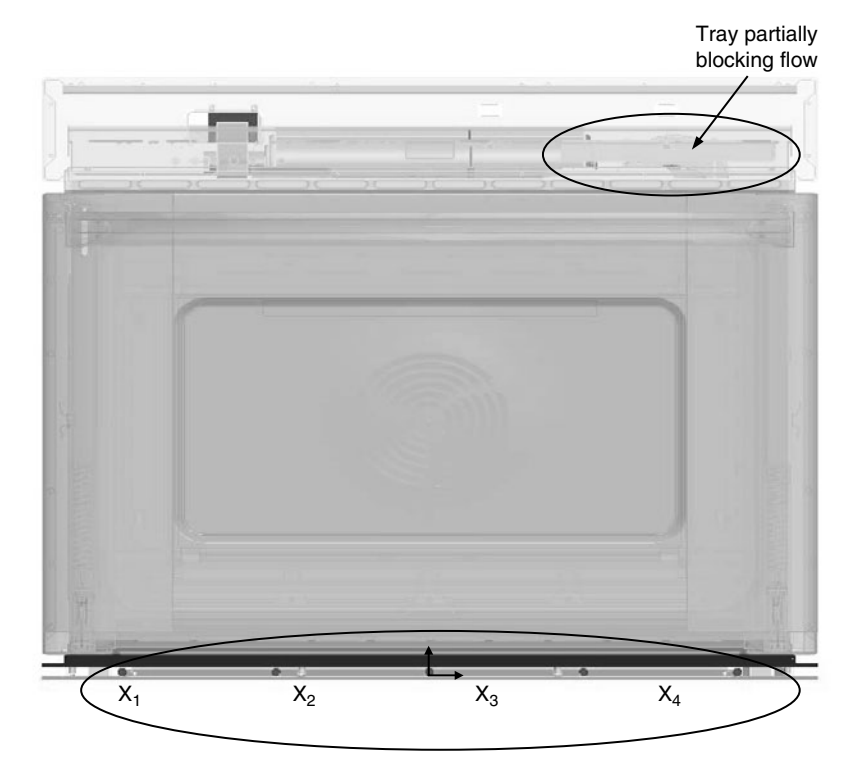


Figure 5 Location of horizontal hot-wire measurements at outlet.

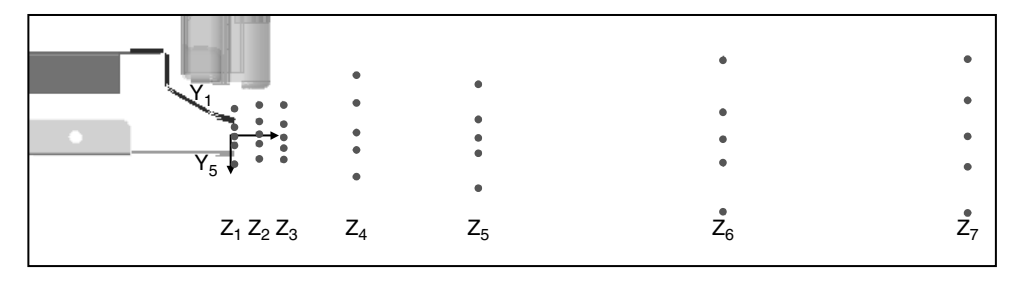


Figure 6 Location of hot-wire measurements in outlet jet.

3.4. NUMERICAL MODELLING

The equations used within this problem are given in equations (1)–(4):

$$\frac{\partial \rho}{\partial t} + \frac{\partial \left(\rho \mathbf{u}_{i}\right)}{\partial \mathbf{x}_{i}} = 0 \tag{1}$$

$$\frac{\partial \left(\rho u_{i}\right)}{\partial t} + \frac{\partial \left(\rho u_{i} u_{j}\right)}{\partial x_{j}} = -\frac{\partial p}{\partial x_{i}} + \frac{\partial}{\partial x_{j}} \left(\mu \left[\frac{\partial u_{i}}{\partial x_{j}} + \frac{\partial u_{j}}{\partial x_{i}}\right]\right) - \frac{\partial}{\partial x_{i}} \left(\frac{2}{3}\mu \delta_{ij} \frac{\partial u_{k}}{\partial x_{k}}\right) + f_{i}$$
(2)

$$\frac{\partial \left(\rho c_{v} T\right)}{\partial t} + \frac{\partial \left(\rho u_{i} c_{v} T\right)}{\partial x_{i}} = \frac{\partial}{\partial x_{i}} \left(\frac{\partial}{\partial x_{i}} T\right) + q_{T}$$
(3)

with the buoyancy force term

$$\mathbf{f}_{\mathbf{b}_{i}} = (\rho - \rho_{\text{ref}})\mathbf{g}_{i} \tag{4}$$

where u_i are the components of the mean velocity vector, ρ is the fluid density, t is time, p is the pressure, μ is the absolute viscosity, f_i is the external body force vector, δ_{ij} is Kronecker's delta. T is the temperature, c_v is the heat capacity at constant volume, k is the thermal conductivity of the fluid and q_T is the body heat source term. The commercial code used in this work, CFX, uses finite volume discritised formulation. The pressure and velocity are decoupled using a single cell, unstaggered, collocated grid to overcome *checkerboard* oscillation issues. Shape functions are used to evaluate the diffusion terms in the governing equations and the pressure gradient term. The advection term is discretised using an upwind formulation. The hydrodynamic equations for velocity and pressure are solved as a single system using a coupled solver that is fully implicit in time. Further details can be found in the CFX manual [12].

Given the complexity of the Titan oven as a thermal system a two-dimensional representation was first trialled. This allowed efficient use of elements for resolving the internal flows in narrow passageways and provided faster feedback than a more computationally intensive three-dimensional model. It was recognised that the two-dimensional approach would possibly be to the detriment of accuracy and would not include some of the characteristics observed in the experimental results. Prior experience indicated the value of starting with a simplified representation and increasing the complexity of the model to address its shortcomings at a later stage if necessary. It was also decided not to model the tangential fan and replace it with an appropriate mass flow boundary condition. Figure 7 shows the geometric

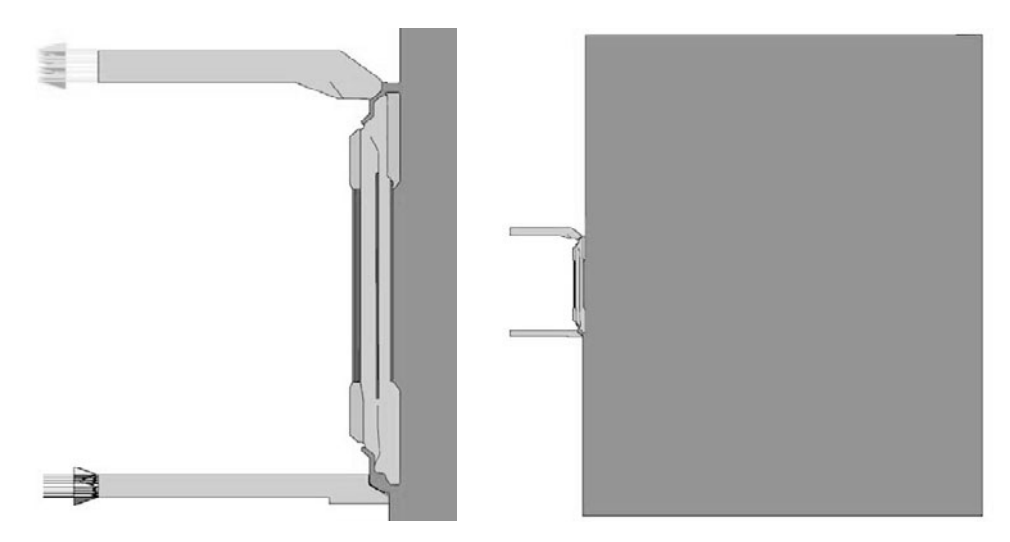


Figure 7 Titan oven cooling circuit, door and room.

Table 1 CFD cases

	Number of elements	Comment
CFD I	370k	Without heat transfer into duct
CFD II	370k	With heat transfer into duct
CFD III	510k	With heat transfer into duct

model with the panes of glass coloured red, the rock wool insulation is coloured grey. Internal air is light blue and the external air in the room that the oven is facing is darker blue.

The fluid was taken as being air as an ideal gas. The full buoyancy model was required to model natural convection because the temperature gradients exceed the recommended range of the Boussinesq buoyancy model. Turbulence was modelled using the SST turbulence model which uses k- ω formulation close to the wall, therefore negating the need for any wall treatment, and k- ε formulation elsewhere. The inlet and outlet in the model were the lower and upper cooling circuit ducts as the fluid in the room was enclosed by walls on all sides. The appropriate mass flow on the inlet and outlet boundaries were set based on the volume flow rate measured but these had to be tuned to account for experimental error. The temperature on the inlet and outlet boundaries, and the temperature on the cavity side of the door were specified from the temperatures measured experimentally with the thermocouples. The temperature boundary condition for the inner surface of the door was created by fitting a second-order polynomial through the three experimental measurements at the top, middle and bottom of the door.

During the experimental work a climate control system removed the heat from the thermodynamic system and maintained the ambient air temperature outside of the oven. As this is impractical and unnecessary to include in the model so a more suitable method was sought. It was found that applying a temperature of -10° C on the ceiling, floor and the wall opposite the oven had the desired effect. Three cases were run as detailed in table 1, with cases I & II having relatively coarse meshes. The first case had no heat transfer from the cavity into the duct which was rectified in case II. Case III was run with the heat transfer into the duct and a finer mesh.

Cases I & II showed results which were invariant with time. When case III was run from scratch the results were inconsistent with those from the experiment, a bifurcation of the solution was encountered. This observation highlighted the fact that there was maybe more than one numerically stable steady state solution. The coarse mesh results were then interpolated onto the fine mesh as initial conditions to trigger the desired solution; the results were then similar to the physical experiment but it was difficult to achieve convergence, with the residuals flattening out and reaching a tolerance of 10^{-4} on the r.m.s of the residuals. This suggests that the solution for case III should be transient but was in this case constrained by the software to be steady state. It could not be run transient due to limitations of time and computing capacity.

4. RESULTS

4.1. FLOW VISUALISATION

Figure 8 gives a still close-up of the inlet between the top of the door and the bottom of the control panel. The fan of laser light is visible and the reflection (dark line) of the front of the oven highlights the inlet with a portion of the door handle also in view. The streak lines

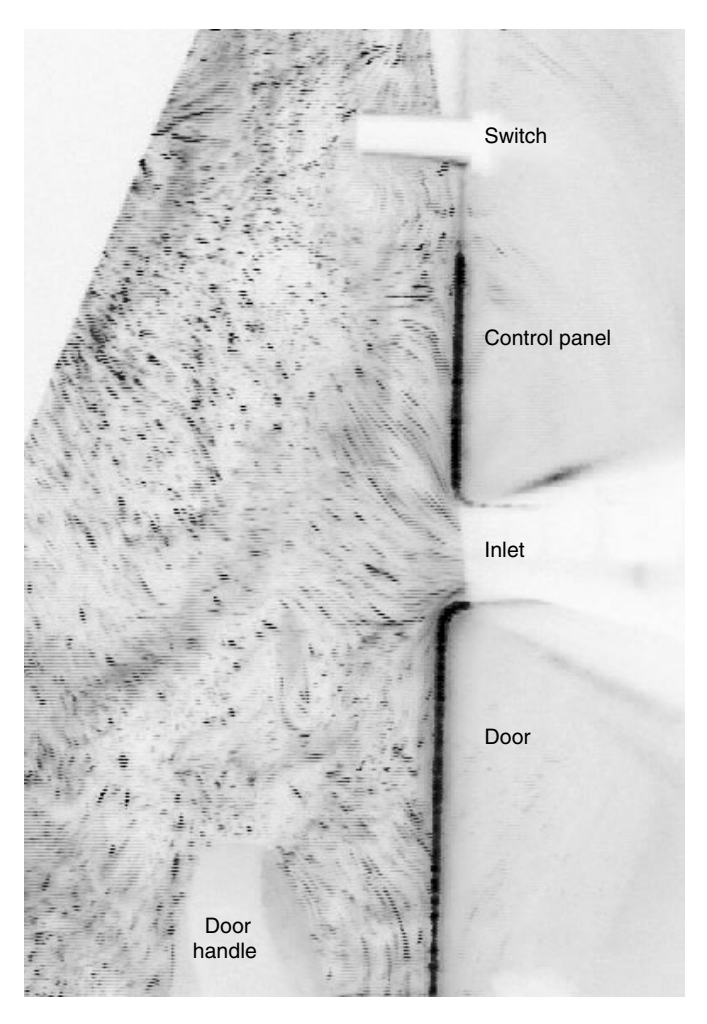


Figure 8 Flow visualisation at the inlet region.

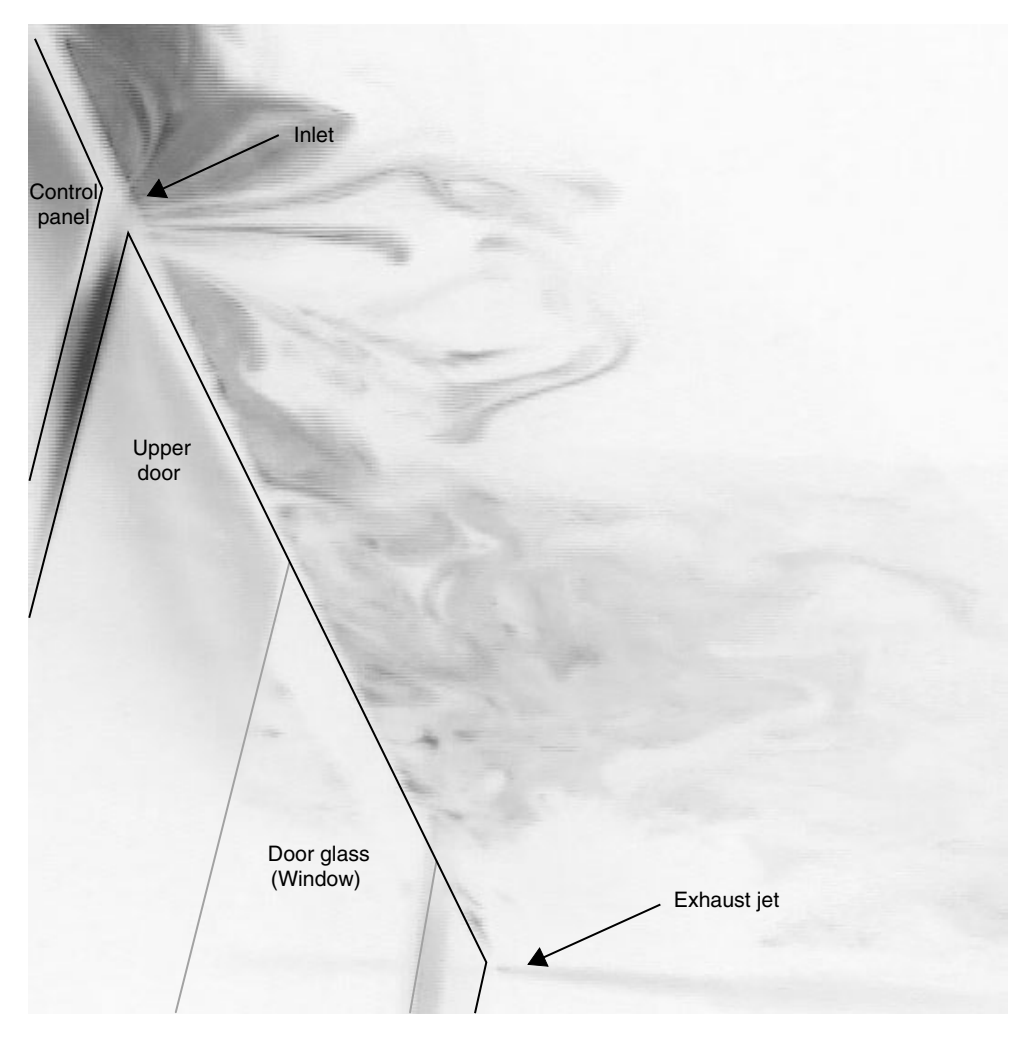


Figure 9 Flow visualisation. Oblique view down the front of Titan oven.

show the flow converging on the inlet. Figure 9 is an oblique view taken from the left-hand side above the oven looking down the front surface. The concentration of smoke in the air can be seen stretching into the inlet with the exhaust jet from the outlet also visible below. From the video footage it was seen that the flow is unsteady and contains numerous large scale eddies. Air is rapidly drawn into the inlet from in front, above and below. Flow can be seen creeping down the lower surface of the door and drawn into the bottom of the door above the jet.

4.2. VELOCITY COMPARISON

As the CFD model was two-dimensional only one of the experimental measurement locations occurred at the outlet, X_3 . Table 2 hows the comparison between this value and the values from the three CFD cases. The value predicted by CFD agrees to within 3% of the experimental value but this of course is by design of the mass boundary condition.

Table 2 Velocity comparison at the outlet

X_3	CFD I	CFD II	CFD III
3.44m/s	3.33m/s	3.34m/s	3.33m/s

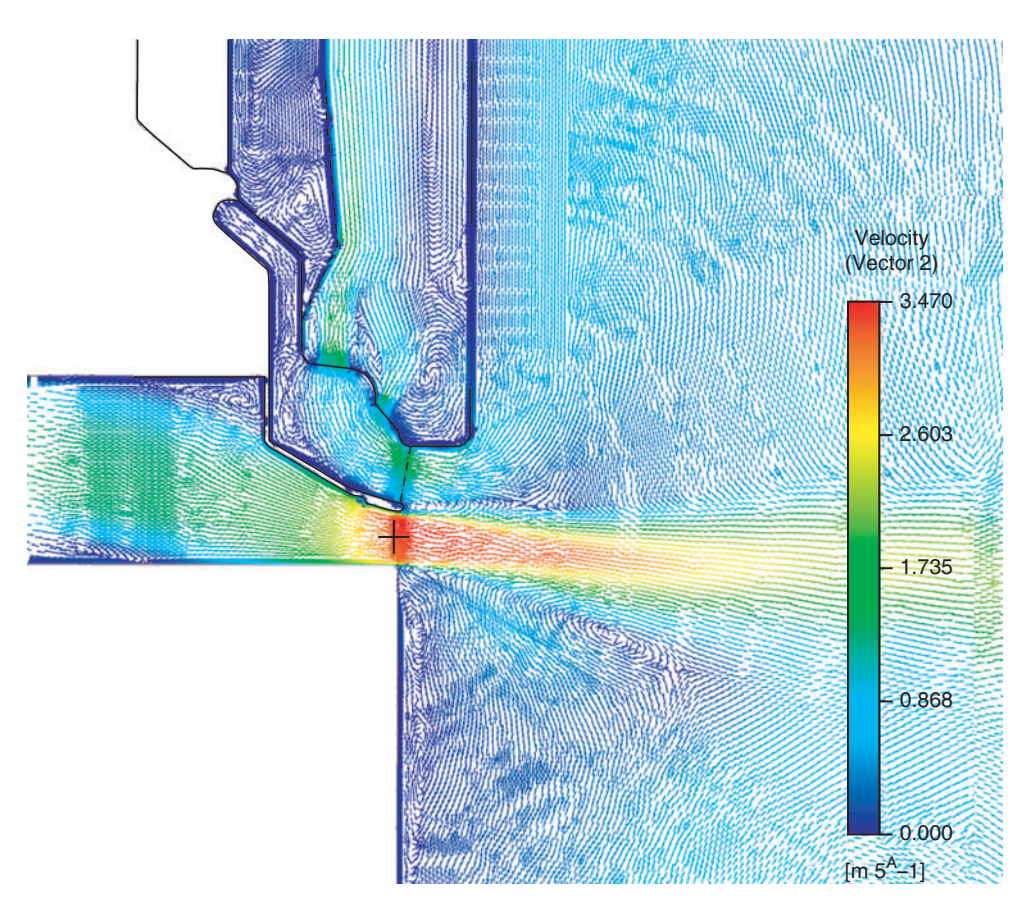


Figure 10 Velocity at cooling circuit outlet.

Figure 10 gives the velocity vectors at the cooling circuit outlet. The behaviour generally matches observations with the slot jet clearly visible and the flow travelling down the front of the door before being drawn into the bottom of the door.

Behind the inlet vent position X_4 is used for comparison with five vertical measurements being taken spread between the ceiling of the duct and the angled deflector plate, figure 11. Table 3 gives the comparison between the measurements and CFD results.

It can be seen that the average is very similar, indicating that the volumetric flow rate is the same. The poorest comparison is with CFD I whilst there is little difference between CFD II & III. Figure 11 shows a large recirculation zone in the upper region of the duct and another smaller one on the front of the deflector. The size and location (if there is a steady location) are likely contributors to the uncertainty of the CFD results. It also highlights that the direction of the velocity vector in relation to the hot wire probe and whether the assumed normal direction is in fact correct.

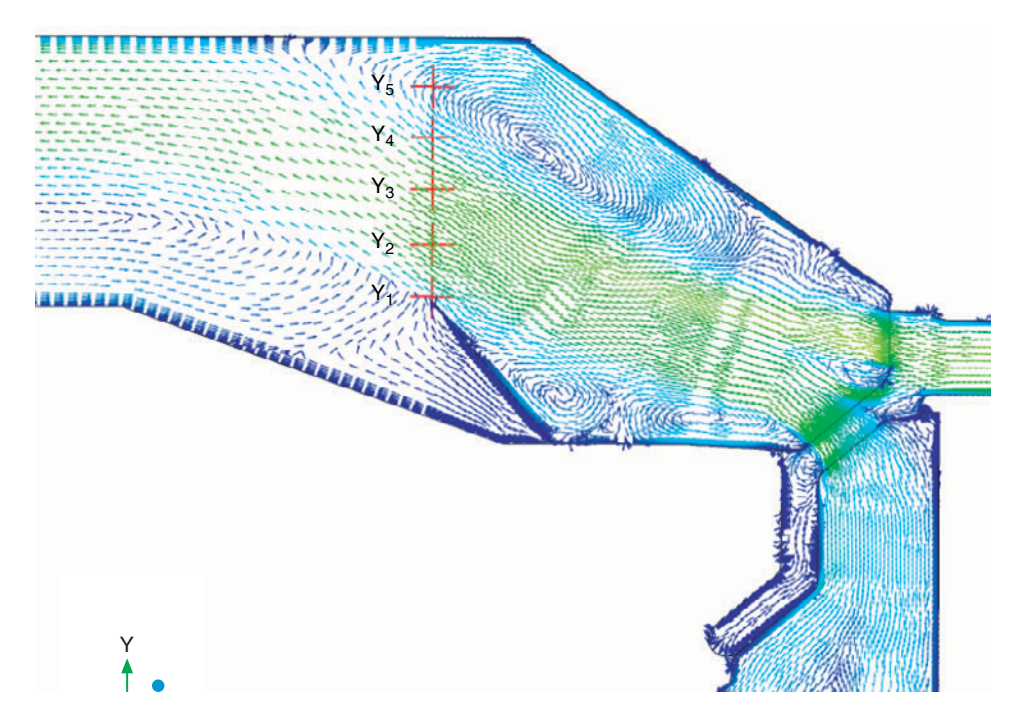


Figure 11 Vertical Locations of Points for Comparison (CFD Case I).

Table 3			

[m/s]	X_4	CFD I	CFD II	CFD III
$\overline{Y_5}$	1.33	0.04	0.70	0.72
\overline{Y}_4	1.70	1.02	1.63	1.45
$\overline{Y_3}$	1.28	1.89	1.95	1.71
\overline{Y}_2	0.55	1.86	0.68	0.84
$\overline{\mathbf{Y}_{1}}$	0.49	0.72	0.30	0.66
Average	1.07	1.11	1.05	1.08

Figure 12 shows the measurement locations overlaid on a vector plot of results from case CFD III for the outlet jet. A number of the hot wire results were known from this to be erroneous due to the flow passing backwards over the probe and measured velocities which are below the calibrated range (less than 0.6m/s). Table 4 distinguishes these by shading the acceptable measurements.

Figure 13 shows the difference between the hot wire and CFD values calculated as a percentage of the hot wire value for case CFD III. Overall there is good agreement in the potential core of the jet. In contrast the entrainment area outside the potential core region shows poor correlation. This is in part a symptom of incomplete convergence and an absence of a steady state solution. Poor agreement does not necessarily mean that the CFD results are wrong, rather that when the flow is unsteady with buoyancy and entrainment there is no single solution.

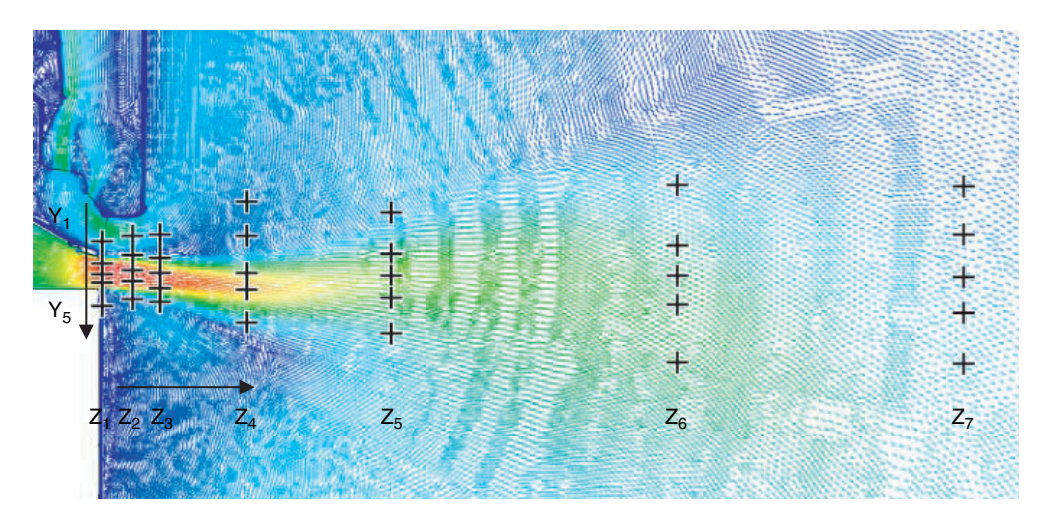


Figure 12 Locations of comparison points.

Table 4 Comparison of hot wire and CFD velocities in outlet jet

[m/s]		\mathbf{Z}_1	\mathbf{Z}_2	\mathbf{Z}_3	\mathbb{Z}_4	\mathbf{Z}_{5}	\mathbf{Z}_6	\mathbf{Z}_7
$\overline{\mathbf{Y}_{1}}$	HW	0.69	0.85	0.62	0.09	-0.08	-0.14	0.00
	CFD I	0.94	1.21	0.53	0.36	0.58	0.73	0.43
	CFD II	0.59	1.29	0.21	0.34	0.65	0.29	0.36
	CFD III	0.99	1.34	1.02	0.32	0.31	0.45	1.42
$\overline{Y_2}$	HW	0.338	0.58	0.69	0.09	0.54	0.52	0.37
	CFD I	3.45	0.32	0.79	0.34	1.59	1.38	0.54
	CFD II	3.54	1.25	2.54	0.95	0.83	0.83	0.52
	CFD III	3.42	0.26	1.19	0.20	1.26	0.53	0.44
$\overline{Y_3}$	HW	3.32	3.20	3.04	1.17	1.08	0.80	0.62
	CFD I	3.35	3.39	3.24	2.37	2.07	1.61	0.65
	CFD II	3.36	3.52	3.37	2.48	0.91	1.09	0.67
	CFD III	3.37	3.49	3.44	3.19	2.27	0.60	0.46
$\overline{Y_4}$	HW	3.34	3.36	3.34	2.71	1.64	1.14	0.89
	CFD I	3.24	3.32	3.10	2.89	1.92	1.68	0.77
	CFD II	3.17	3.25	2.29	2.59	1.19	1.20	0.80
	CFD III	3.32	3.48	3.22	2.38	2.46	0.74	0.48
$\overline{Y_5}$	HW	-0.59	0.14	1.67	1.36	1.82	1.40	1.09
	CFD I	0.05	0.21	0.77	0.82	1.23	1.59	0.91
	CFD II	0.06	0.27	0.59	0.82	1.81	1.09	0.94
	CFD III	0.15	0.21	0.10	0.43	1.00	1.25	0.50

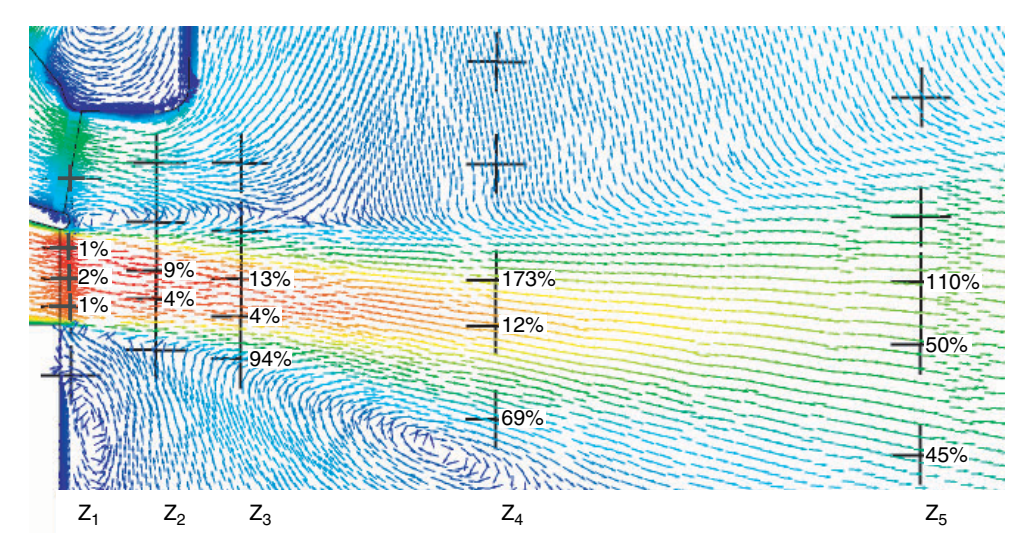


Figure 13 Velocity difference at comparison points, CFD III and hot-wire.

Rather than prove the superiority of one method over the other the comparison highlights the limitations of both CFD and the hot wire results. From an engineering value perspective both sets of results are valuable as they provide information about the fluid behaviour. Encountering partial and conflicting information is not uncommon in engineering and filtering this is vastly preferable to working with no information. This viewpoint highlights the use of CFD for provoking thought and the synergy between the numerical and experimental approaches.

4.3. TEMPERATURE COMPARISON

Of the 59 thermocouple measurements taken, 31 coincide with locations in the twodimensional CFD model. Figure 14 shows the location of these points overlaid on a temperature contour plot. Table 4 gives the temperature differences (calculated as a percentage in Kelvin) with the thermocouple.

Overall the agreement between the temperatures predicted by CFD and the measured values is reasonably good. It can be seen in CFD I the effect of the incorrect boundary condition is a higher average difference compared with CFD II and CFD III. In the finer mesh model of CFD III more than half of the temperatures are within ± 10 K of the measured value.

The locations that compare poorly may be due to simplifications in all the model which compromise accuracy such as; the 2D approximation, neglecting the sheet-metal that encases the insulation in the door, and explicitly modelling the oven cavity. The modelling of the insulation is likely to be the cause of the largest absolute temperature difference at location 15 (the CFD over predicts the temperature). Nearby locations 13, 17 and 26 have relatively small differences. In reality the insulation is situated within the sheet metal internal structure of the door. The sheet metal has large effect on the lateral heat transfer on the fluid-solid interface surface but was impractical to include in the CFD model without shell type elements.

Point 25 also compares poorly and is located in a high thermal gradient area. Moving the comparison point slightly in the CFD model has a large influence on the temperature. The difference is therefore very sensitive to the precise position of the thermocouple and the point chosen for comparison in the CFD model.

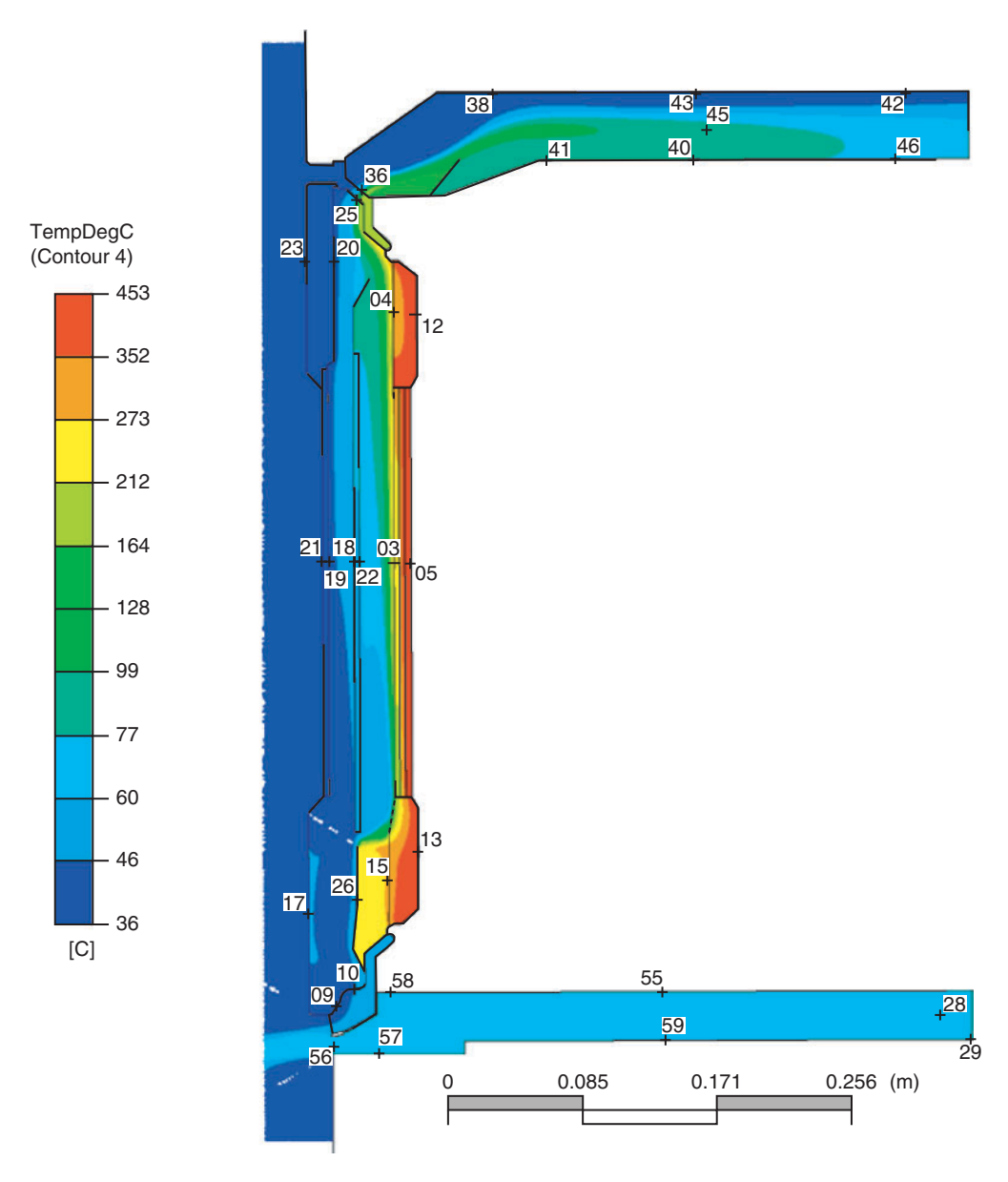


Figure 14 Temperature comparison points overlaid on CFD model.

The temperatures on the glass pane at locations 18 and 22 are also relatively poor (all under predicted by the CFD). This may be a consequence of the 2D approximation, where heat is only transferred to this glass pane in the CFD model by the convecting air. In reality the glass pane is secured to the internal structure of the door and heat will be transferred to the glass by conduction through this connection.

Overall as a model for predicting temperature distribution within the Titan oven cooling circuit and door the CFD model is more than satisfactory. The three temperatures on the outside surface of the door at locations 23, 21 and 17, critical design values with regard to

Table 5 Temperature comparison between Experimental and 3 CFD cases

Location	$CFDI$ $\Delta[K]$	CFD I Δ[%]	$CFD~II$ $\Delta[K]$	CFD II $\Delta [\%]$	CFD III $\Delta[K]$	CFD III $\Delta [\%]$
03	-17.5	-3	-23.9	-4	-17.8	-3
04	-27.2	-5	-34.0	-6	-26.9	-5
05	0.2	0	0.2	0	0.2	0
09	1.1	0	17.4	5	19.2	6
10	-6.5	-2	23.1	7	23.6	7
12	-1.4	0	-1.5	0	-1.5	0
13	21.1	3	21.1	3	21.1	3
15	102.6	21	124.6	26	112.4	24
17	5.5	2	5.4	2	4.2	1
18	-66.1	-17	-71.3	-18	-69.1	-17
19	-0.2	0	-1.9	-1	-2.9	-1
20	-68.5	-18	-67.4	-18	-69.3	-18
21	1.4	0	0.1	0	-0.9	0
22	-74.6	-18	-79.7	-20	-77.6	-19
23	3.8	1	2.0	1	1.1	0
25	-89.5	-20	-94.2	-21	-96.5	-21
26	13.6	4	17.2	6	8.5	3
28	4.8	1	1.3	0	1.2	0
29	14.6	4	11.1	3	11.0	3
36	-51.0	-13	-55.8	-15	-55.8	-15
38	-12.7	-4	-7.1	-2	-6.9	-2
40	-44.4	-11	0.9	0	0.7	0
41	-52.5	-13	-2.6	-1	-2.1	-1
42	-12.1	-4	-3.8	-1	-2.9	-1
53	-12.8	-4	-4.0	-1	-4.8	-1
45	10.2	3	16.7	5	20.2	6
46	-47.5	-12	-5.8	-1	-6.5	-2
55	-29.3	-8	-1.5	0	-1.0	0
56	1.4	0	29.1	8	29.6	9
57	13.0	4	2.0	1	1.6	0
58	-54.2	-14	-51.8	-14	-55.9	-15
59	14.3	4	2.1	1	1.9	1
4	-14.4	-4	-7.2	2	-7.6	2
Average	-14.4	-4	-1.2	-2	-/.0	-2

safety standards, compare well. Having established an awareness of the limitations and strengths of CFD and confidence in the model it can now be used as a design tool for testing alternative configurations of the Titan oven door. Work can therefore take place for consequent evolutions of the oven design and more of an optimal solution possibly found for the cooling of the oven door.

5. DISCUSSION

Prior to this work relatively little was known about the performance of the Titan oven door, other than it took a considerable amount of prototype testing to pass safety standards. The results of this modelling and the extensive measurements provide significantly deeper insight into the design. As a design tool the model would allow alternative design configurations to be tested for a fraction of time and cost of prototyping. This allows safer and more energy efficient products to be developed by finding the optimal thermal performance. Most importantly it went most of the way to answer the questions posed by the design engineers during the development of the project regarding the flow of air at the inlet and outlet of the cooling circuit. This was a positive benefit of using CFD within the product development process.

The decision to model the flow in 2D has been vindicated by comparison with the experimental data. The comparisons with temperature were particularly good as were the velocity comparisons in the inlet duct and at the outlet vent. It is difficult to achieve good agreement in areas where the flow was unsteady, for example as a result of buoyancy and entrainment. Optimally a 3D simulation would be desirable but practical limitations clearly exist for solving such a model. Furthermore the 2D model requires less time to construct and is far easier to modify when testing design variations. Such a decision could not have been made without the use of extensive experimentation and flow visualisation. In the future for a similar situation that knowledge will allow informed and intelligent decisions to be made as to whether continuing validation is necessary or if there is sufficient confidence in the CFD to trust the results to help make design decisions. In situations, such as this, CFD has provided insight into a flow of which little was known. This has provided the design and engineering team with information that will inform the design of future ovens.

No change was apparent in the results of CFD III that could be attributed to the finer mesh. Differences in CFD II and III are more likely due to the lack of an unsteady state solution and the consequently incomplete convergence. The improvement between CFD I, II and III highlights the need for correct boundary conditions. The finer mesh, case CFD III, triggered a bifurcation which is an indication of a potentially unsteady solution. Therefore although the coarse mesh simulations converged more easily there is a danger of missing potential unsteadiness without the finer mesh.

This study highlights how CFD accuracy can be enhanced by including experimental information into the boundary conditions. The CFD revealed characteristics and properties of the flow that are useful in the experimental investigations. In this case the CFD showed that the assumption about the orientation of the flow relative to the hot wire probe used to take velocity measurements was unsafe.

6. CONCLUSIONS

The following conclusions can be made from this work:

- The velocities predicted by CFD compared reasonably well with the hot wire measurements behind the inlet vent and in the potential core of the jet at the outlet vent.
- The air entrained in the outlet jet did not compare well due to its unsteady nature. The results indicate that there is very little recirculation of the flow from the outlet jet into the door.
- The CFD model predicted temperatures to within 3% of the measured temperatures in most locations
- The oven cooling circuit was doing the job it was designed for but that was more by luck than through sound fluid and thermal knowledge and understanding

- The CFD analysis gave the oven development team a much better understanding of the behaviour of the flow through the Titan oven door and cooling vents. The model could be used to test alternative designs that would otherwise need to be prototyped.
- There was a synergy between the CFD, experimental measurements and flow visualisation that allowed a holistic understanding of the flow situation that enhanced each of the three aspects of investigation
- Establishing a CFD methodology within the product design process of an industry allows the exploration of the design space in terms of safety and energy efficiency.

REFERENCES

- B. Dabell, C. Musiol and M. Pompetzki, The Benefits of Computer Aided Engineering, in J. H. Edwards and P. E. J. Flewitt ed(s), Fifth International Conference on Engineering Structural Integrity Assessment, 2000.
- [2] UL 858, Standard for Safety Household Electric Ranges.
- [3] AS/NZS3350.2.6:1998 (IEC 60335-2-6-1997), Safety of Household & Similar Electrical Appliances. Part 2.6 Particular Requirements Stationary Cooking Ranges, Hobs, Oven & Similar Appliances.
- [4] P. Verboven, N. Scheerlinck, J. De Baerdemaeker and B. M. Nicolai, Computational Fluid Dynamics Modelling and Validation of the Isothermal Airflow in a Forced Convection Oven, *J. Food Engineering*, 2000, 43 41–53.
- [5] P. Verboven, N. Scheerlinck, J. De Baerdemaeker and B. M. Nicolai, Computational Fluid Dynamics Modelling and Validation of the Temperature Distribution in a Forced Convection Oven, J. Food Engineering, 2000, 42 61–73.
- [6] P. Gerhardinger, Next Generation Heated Glass Products for Food Service Appliances, in ed(s), 54th International Appliance Technical Conference, 2003.
- [7] T. Sümer, E. Dirik, Ö. Akbas and A. Kara, Thermal Analysis and Simulation of an Electric Oven, 45th IATC, 1994.
- [8] R. P. Lovingood, E. A. De Merchant and L. J. Himes, Oven Performance In Convention vs. Radiant Mode, 45th IATC, 1995.
- [9] C. Aydin, E. Dirik, T. Sümer and M. Y. Tanes, Computational Analysis of Flow Characteristics In an Oven, 46th IATC, 1995.
- [10] D. Ward, Basic Thermal Modeling of Oven Cooking and the 'Brick' Test, 53th International Appliance Technical Conferences, 2002.
- [11] A. Kayôhan, B. Özyurt and C. Inan, A Method for Determining the Heat Loss Characteristics of an Oven, 54th International Appliance Technical Conferences, 2003.
- [12] ANSYS Inc, CFX-5.7.1 Theory Manual, ANSYS, 2005.
- [13] R. Subrata, K. Sagar and J. Heidmann, Film Cooling Analysis Using DES Turbulence Model, in *ASME Turbo Expo*, 2003.
- [14] K. K. Dhinsa, C. J. Bailey and K. A. Pericleous, Turbulence Modelling and its Impact on CFD Predictions for Cooling of Electronic Components, in *Inter Society Conference on Thermal Phenomena*, 2004.
- [15] J. C. S. Lai and C. Y. Yang, Numerical Simulation of Turbulence Suppression: Comparisons of the Performance of Four k-e Turbulence Models, Int. J. Heat and Fluid Flow, 1997, 18 575–584.
- [16] WS Atkins Consultants, Best Practice Guidelines for Marine Applications of Computational Fluid Dynamics, 2002.
- [17] D. C. Wilcox, Basic Fluid Mechanics, D C W Industries, La Canada, 1998.
- [18] F. R. Menter, Two-Equation Eddy-Viscosity Turbulence Models for Engineering Applications, AIAA Journal, 1994, 1598–1605.
- [19] F. R. Menter, Zonal Tow-Equation k-w Turbulence Models for Aerodynamic Flows, AIAA Paper, 1993.

- [20] F. R. Menter, A Comparison of Some Recent Eddy-Viscosity Turbulence Models, *Transactions on the SNAME*, 1996, 118 514–519.
- [21] F. R. Menter and M. Kuntz, Development and Application of a Zonal DES Turbulence Model for CFX-5, 2003.
- [22] K. McEwen, APPS499 Report, 2005.

ACKNOWLEDGEMENTS

The authors gratefully acknowledge the assistance of Fisher & Paykel Appliance Ltd. and the Foundation for Science Research and Technology, Contract Number FSPX0001.